

Batchelor Scaling in Fast-Flowing Soap Films

Y. Amarouchene and H. Kellay

Centre de Physique Moléculaire Optique et Hertzienne, Université Bordeaux I, 351 cours de la Libération, 33405 Talence France
(Received 9 June 2004; published 19 November 2004)

The dynamics of a passive scalar such as a dye in the far dissipative range of fluid turbulence is a central problem in nonlinear physics. An important prediction for this problem was made by Batchelor over 40 years ago and is known as Batchelor's scaling law. We here present strong evidence in favor of this law for the thickness fluctuations in the flow of a soap film past a flat plate. The results also capture the dissipative range of the scalar which turns out to have universal features. The probability density function of the scalar increments and their structure functions come out in nice agreement with theoretical predictions.

DOI: 10.1103/PhysRevLett.93.214504

PACS numbers: 47.27.Ak, 47.27.Gs, 47.27.Jv, 68.15.+e

How pollutants, chemicals, or nutrients are mixed at the smallest scales of turbulence, which is ubiquitous in industrial and natural settings, is of practical and fundamental importance. The crucial steps towards solving this problem were exposed by Batchelor in a seminal paper dating back to 1959 [1]. He considered the dynamics of a passive scalar θ (such as temperature or concentration) for scales smaller than the velocity dissipation scale r_K . The velocity field consists of random straining motion in the dissipative range of fluid turbulence where the energy density spectrum decays exponentially [2]. The scalar θ is assumed to have no backreaction on the flow and to obey a convection-diffusion equation: $\partial\theta/\partial t + \mathbf{v} \cdot \nabla\theta = \kappa\nabla^2\theta$, where \mathbf{v} is the velocity field obeying the Navier-Stokes equations and κ is the diffusivity. The dissipation scale r_B of the scalar is assumed to be much smaller than r_K . Basically, the scalar is subject to random stretching and folding which end up creating small-scale inhomogeneities down to the scale r_B . The spectral density $E_\theta(k)$ of the scalar θ was predicted by Batchelor to be $E_\theta(k) = \chi(\gamma k)^{-1} \exp(-\frac{\kappa k^2}{\gamma})$, where χ is the scalar dissipation rate and γ is the effective strain rate; the spectral density is defined such that $\langle\theta^2\rangle = \int_0^\infty E_\theta(k)dk$ (where $k \sim 1/r$ is the wave number or inverse length scale). The exponential factor is due to the dissipation of the scalar and operates at scales smaller than r_B while the k^{-1} factor is the Batchelor scaling law valid in the viscous-convective range located at scales $r_K < r < r_B$. Fluctuations in the rate of strain led Kraichnan [3] to propose other forms for the scalar dissipation. The simplest one suggests that the exponential factor above is replaced by $\exp[-(c\kappa/A)^{1/2}k]$, where c is a numerical constant and A is a strain rate. Thus, the k^{-1} scaling survives, but the dissipation part is replaced by a more gentle decay. Recent analytical developments [4,5] confirm Batchelor's k^{-1} scaling law and predict the variation of the structure functions of scalar increments versus the scale r . These increments on a scale r are defined as $\delta\theta(r) = \theta(x+r) - \theta(x)$ and the second-order structure function is given by

$\langle\delta\theta^2(r)\rangle \sim \log(r)$ [5], where the brackets indicate an ensemble average. The probability distribution function (PDF) of $\delta\theta(r)$ is predicted to have an exponential tail.

On the experimental side, and despite the importance of these results, no consensus exists as to their validity [6,7]. While some experiments in three dimensions [8] did find the Batchelor scaling law, others did not [9] and the reasons for such a divergence are still not clear. In two dimensional flows, Wu *et al.* [10] found good evidence for the k^{-1} scaling law but Williams *et al.* [11] did not. Clearly more experimental work is needed [6] to elucidate the validity of the above-mentioned theoretical results. The behavior of a scalar field in a smooth random velocity field, which is the case for the dissipative range of fluid turbulence, is one of the few problems in nonlinear physics that is well understood theoretically [4,5].

Measurements done in a two dimensional enstrophy cascade range [12,13] did find a k^{-1} scaling law for the passive scalar spectral density. Since the energy density spectrum in these experiments scales as k^{-3} , the velocity field in this case is smooth and a k^{-1} scaling law is again expected [4]. The dissipative range of the scalar was not resolved in these experiments. Although these results confirm the k^{-1} scaling for a particular case valid in 2D, they are not experimental tests of Batchelor's scaling law in the viscous-convective range where the energy density spectrum decreases exponentially versus the wave number, a more general case of a smooth velocity field.

Herein, we report extensive measurements of passive scalar statistics taken in a fast-flowing soap film, a good model for 2D flows [14]. Soap films have a thickness of order a few microns so the velocity field is confined to the plane of the film and the vorticity is essentially perpendicular to the film plane. The thickness of these flowing soap films gets modulated by the velocity variations as has been demonstrated on numerous occasions [13–15]. The fluctuations in thickness h in flowing soap films behave as a passive scalar [10,13,15] and are believed to be governed by an equation similar in essence to the usual convection-diffusion equation but with a different dissi-

pative term: $\partial h/\partial t + \mathbf{v} \cdot \nabla h = -\kappa' \nabla^4 h$, where κ' (dimensions cm^4/s) is the analog of the diffusivity and \mathbf{v} is the two dimensional velocity field [10,16]. We here present strong evidence for Batchelor's scaling law for the spectral density of the film thickness fluctuations with the expected logarithmic variation of the structure functions versus the scale r in the viscous-convective range. The small-scale end of the measured scalar spectral density varies exponentially versus the wave number k in agreement with Kraichnan's prediction.

The experiments use rapidly flowing soap films [14] contained between two nylon wires 5 cm apart; the total length of the film is 2 m [see Fig. 1(a) for a schematic of the flow configuration]. Since the soap solution (water with 1% detergent) was brought to the top of the channel with a micropump, the soap film was constantly replenished. The soap film flowed down with speeds U_f between 1 and 3 m/s. The results presented here are for $U_f = 160 \text{ cm/s}$ with a mean film thickness of $3 \mu\text{m}$. A flat plate with a side of 2 cm was then inserted perpendicularly to the film either at the center of the channel or near one of the nylon wires. The recirculation region behind the flat plate is shown in Fig. 1(b) and consists of a relatively large region with clearly visible thickness variations, as indicated by the different interference colors, and important velocity fluctuations. This is the region where the measurements of the thickness fluctuations and the velocity fluctuations are carried out. We usually chose a region where a mean flow is well established. We used laser doppler velocimetry for the velocity measurements in both the longitudinal and transverse directions. The soap solution was seeded with $0.3 \mu\text{m}$ latex beads. The thickness measurements were carried out using a

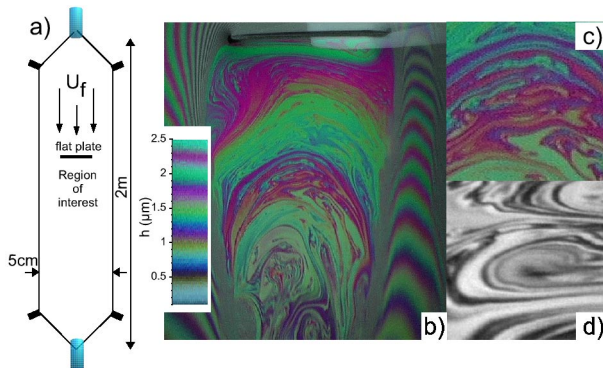


FIG. 1 (color online). (a) A schematic of the setup. The flat plate was inserted perpendicularly to the film plane and is indicated by the thick solid line. The film is replenished by a micropump pumping water from a reservoir of soap water placed at the bottom of the film to the top of the channel. Photographs of the wake in reflection from a white light source: (b) full area, (c) a zoom on a 1 cm^2 region, and (d) monochromatic light image [same area as (c)]. The color bar indicates film thickness in μm .

homemade interferometer [13,15] which uses a piezoelectric transducer on one of the arms and a feedback loop to maintain the two arms at the same phase shift. Changes of the thickness induce changes of this shift which are then compensated by small displacements of the transducer: the voltage driving the transducer is linearly proportional to the thickness fluctuations. The interferometer allowed frequencies as high as 4 kHz with a resolution of order a few nanometers for the thickness variations. Since measurements are carried out at one point where a time series of the thickness fluctuations or the velocity fluctuations is measured, the Taylor hypothesis is used to convert time scales to length scales ($r = U/f$, where U is the mean velocity and f is the frequency). This is the reason we measured these fluctuations in regions where a mean flow is well defined. The time series of these fluctuations are then Fourier analyzed to obtain the power spectra. Besides these temporal measurements, we also analyzed the spatial thickness field through interference images which are then converted to the film thickness as in the experiments of Wu *et al.* [10]. From such fields, the spatial Fourier transforms of the thickness field are obtained and the spectral density can be calculated. Such spatial measurements allow a direct test of the validity of the Taylor hypothesis used in the one point measurements and allow assessment of isotropy.

Typical power spectra and PDFs of the measured velocity fluctuations are shown in Fig. 2. For this location, the longitudinal component has a well defined mean at around $U = 8 \text{ cm/s}$. The transverse component V is centered around 0 cm/s . The low frequency part of the spectra (below 8 Hz) shows anisotropy; the spectral content of the two components is different with more fluctuations in the flow direction. Note that above about 10 Hz, the spectrum decreases nearly exponentially giving a well defined frequency cutoff f_K for the velocity fluctuations:

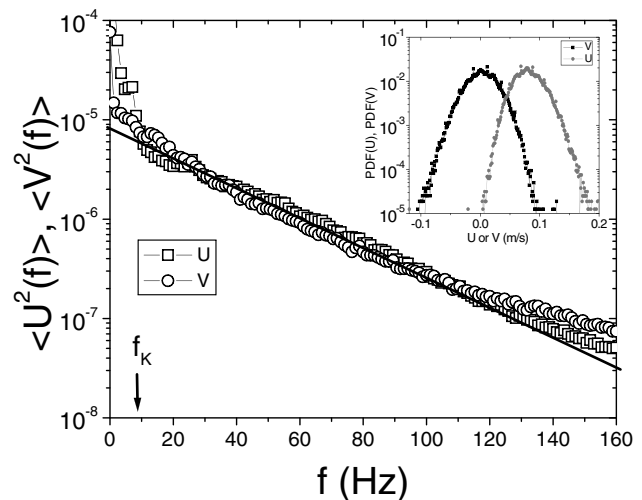


FIG. 2. Velocity power spectra versus the frequency. Inset: PDFs of the velocity fluctuations.

the one dimensional velocity power spectra $\langle U^2(f) \rangle$ and $\langle V^2(f) \rangle$ vary as $\exp(-f/f_K)$. Both velocity components have nearly equal spectral amplitude indicating relatively good isotropy, a necessary condition for Batchelor's argument. Also, this small-scale part of the velocity spectra was roughly similar as we varied the measurement position indicating that the flow is roughly homogeneous. Using the value of f_K , the dissipative scale for the velocity is $r_K = 1$ cm.

Figure 3 shows the one dimensional thickness power spectrum $\langle h^2(f) \rangle$ taken at a position where the velocity has been measured. The spectrum extends from 1 Hz up to 1 kHz. A steep decrease occurs at frequencies higher than about 100 Hz. Below this frequency, a clear scaling range is seen for over a decade. The solid line through the data points is a fit using $k^{-1} \exp(-k/k_B)$. The exponential factor controls mostly the high frequency end with $r_B = 2\pi/k_B = 0.9$ mm. The k^{-1} factor is Batchelor's scaling law. The observation of the k^{-1} scaling is in agreement with the measurements of Wu *et al.* [10]. Note that the k^{-1} scaling extends down to a few hertz and therefore to values below 1 cm, the estimated velocity dissipation scale. This observation has been made before in 3D measurements and 2D simulations [8,17]. The large scale part may well correspond to a chaotic flow which also shows a k^{-1} scaling law [18]. Still there is a region of about one full decade between r_K and r_B corresponding to our viscous-convective range, where the scalar spectrum shows agreement with the k^{-1} scaling law while the velocity spectrum decays exponentially. Another inter-

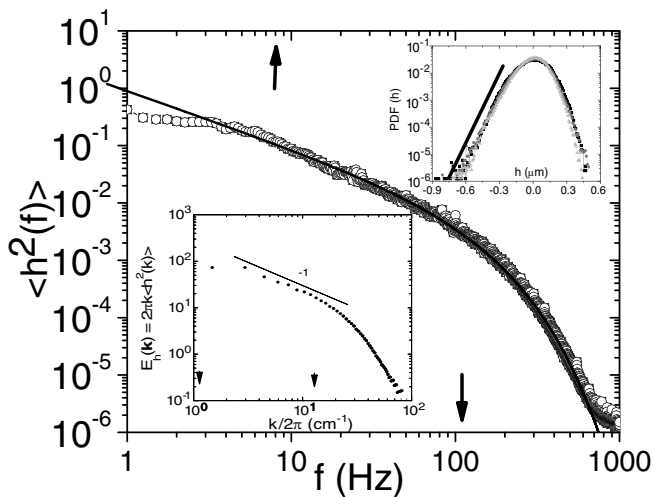


FIG. 3. Thickness fluctuation spectrum from the temporal measurements. The left arrow indicates the position of f_K and the right arrow indicates the position of the frequency corresponding to r_B . Upper inset: probability density functions of the thickness fluctuations relative to the mean thickness which is $1.5 \mu\text{m}$. Lower inset: $E_h(k)$ from spatial measurements using reflection from a sodium lamp. The left and right arrows indicate the k values corresponding to r_K and r_B , respectively.

esting feature of these measurements is shown in the upper inset to Fig. 3. Here, the probability density functions of the thickness fluctuations clearly show an asymmetry towards thicknesses smaller than the mean for which the PDFs have exponential tails which are expected in this regime [4]. These temporal measurements have been complemented by spatial measurements of the thickness field from interference images, such as the one in Fig. 1(d), using monochromatic light from a low pressure sodium lamp. In most of this wake, the thickness variations are relatively small so regions up to 0.9 cm by 0.9 cm can be analyzed where no interference order change occurs and for which the thickness variations do not exceed $0.1 \mu\text{m}$. This was confirmed by visually inspecting color images of this region using a broad white light source [see Figs. 1(b) and 1(c)]. Under such conditions, interference images taken with monochromatic light can be directly converted to the thickness field since the reflected intensity variations are proportional to the thickness variations [10]. This has also been tested by converting the color images to a thickness field using a suitable calibration [see Fig. 1(b)]. Through Fourier analysis of these images (of dimension 512 by 512 pixels so windowing effects are minimal), the scalar spectral density $E_h(k) \sim kh^2(k)$ can be obtained. The spectral density from the color images agrees with that from the monochromatic images but was a little more noisy at high wave numbers. The lower inset of Fig. 3 shows this density $E_h(k)$ versus the wave number extracted from the monochromatic light images. Both the k^{-1} scaling and the exponential decrease ($2\pi/k_B = 0.8$ mm) at small scales are clearly evidenced here in very good agreement with the temporal measurements. Isotropy was checked directly by taking cuts along different angular directions and by directly inspecting the 2D spectrum.

According to Batchelor's original calculation, the dissipation term is $\exp[-(k/k_d)^2]$, where the scalar dissipation wave number $k_d = \sqrt{\gamma/\kappa}$. For the soap film and using the expressions proposed by Wu *et al.* [10,16], the dissipation is expected to vary as $\exp[-(k/k'_d)^4]$ where the dissipation wave number $k'_d = (\gamma/\kappa')^{1/4}$ [10]. Neither experiments nor numerical simulations (except for those of Gotoh *et al.* [17]) have shown these dependencies. Our experiments show that the dissipative part of the scalar varies as $\exp(-k/k_d)$ ($k_d = k_B$: the scalar dissipation scale identified above). The numerical calculations of Ref. [18] also give an exponential decay, $\exp(-k/k_d)$, for the dissipative part rather than the expected term $\exp[-(k/k_d)^2]$. It was argued in [18] that this latter functional form may be masked by intermittency of the stretching rates present giving rise to a slower roll-off at the high wave number end as suggested by Kraichnan. Similar observations of the exponential decay, $\exp(-k/k_d)$, were made in the numerical simulations of Refs. [19,20]. Our experiments agree with these numeri-

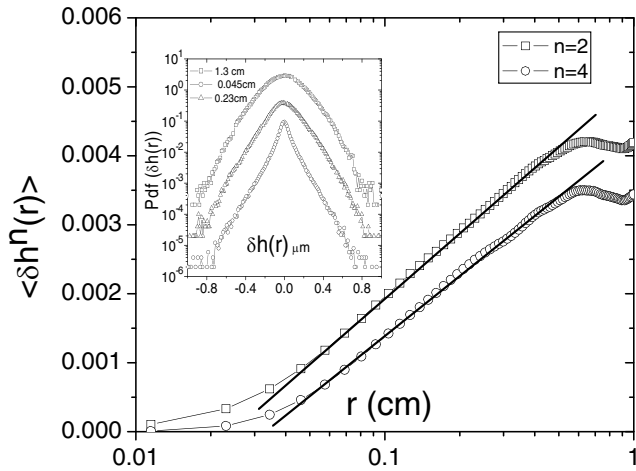


FIG. 4. (a) Second- and fourth-order structure function of the scalar increments in a linear-log plot. (b) PDFs of the scalar increments for different spatial scales r . The PDFs were translated upwards from each other for better visibility.

cal results and may point to the universality of the dissipative range.

A further test of the validity of Batchelor's scaling law in our experiments comes from examining the statistics of scalar increments. The PDF of these increments, $\text{PDF}[\delta h(r)]$, is nearly exponential of the form $\exp[-|\delta h(r)|/\delta h]$ as expected theoretically [4,5]. These are shown in the inset to Fig. 4. Here we have plotted different values of the increment r which are in the dissipative range of the scalar, within the viscous-convective range and at larger scales. While the PDFs for the smaller scales show nice exponential tails, the PDF for the largest scale becomes more Gaussian. Exponential PDFs for the thickness or scalar field increments in the Batchelor regime and at scales smaller than the dissipative scale of the scalar clearly indicate the presence of very large fluctuations. The second-order moment of the thickness increments $\langle \delta h^2(r) \rangle$ is in good agreement with the predictions [4,5] showing a very clear logarithmic variation, $\langle \delta h^2(r) \rangle \sim \log(r)$, as seen in Fig. 4. This variation is seen for scales between 0.6 and 6 mm which coincides with the viscous-convective range determined from the spectral measurements. The fourth-order moment also shows a logarithmic variation versus r (Fig. 4) in agreement with the predictions of Ref. [21] for the range of scales explored here. At smaller scales, the second-order structure function increases roughly as r^2

in agreement with the exponential decrease of the spectral density at small scales.

In conclusion, we have presented strong evidence for the existence of Batchelor's scaling law in the wake of a flowing soap film past a flat plate. This scaling range is then terminated with an exponentially decaying regime signaling the scalar dissipative range which seems to have universal features. The results support recent theoretical work and are in agreement with previous experiments and numerical simulations.

-
- [1] G. K. Batchelor, *J. Fluid Mech.* **5**, 113 (1959).
 - [2] S. B. Pope, *Turbulent Flows* (Cambridge University Press, Cambridge, 2000).
 - [3] R. H. Kraichnan, *Phys. Fluids* **11**, 945 (1968).
 - [4] G. Falkovich, K. Gawedzki, and M. Vergassola, *Rev. Mod. Phys.* **73**, 913 (2001).
 - [5] G. Falkovich and V. Lebedev, *Phys. Rev. E* **50**, 3883 (1994).
 - [6] Z. Warhaft, *Annu. Rev. Fluid Mech.* **32**, 203 (2000).
 - [7] M. Holzer and E. D. Siggia, *Phys. Fluids* **6**, 1820 (1994).
 - [8] H. L. Grant *et al.*, *J. Fluid Mech.* **34**, 423 (1968); J. O. Nye and R. S. Brodkey, *J. Fluid Mech.* **29**, 151 (1967); C. H. Gibson and W. H. Schwarz, *J. Fluid Mech.* **16**, 365 (1963).
 - [9] A. E. Gargett, *J. Fluid Mech.* **159**, 379 (1985); P. L. Miller and P. E. Dimotakis, *Phys. Fluids* **3**, 1156 (1991); P. L. Miller and P. E. Dimotakis, *J. Fluid Mech.* **308**, 129 (1996).
 - [10] X. L. Wu *et al.*, *Phys. Rev. Lett.* **75**, 236 (1995).
 - [11] B. S. Williams, D. Marteau, and J. P. Gollub, *Phys. Fluids* **9**, 2061 (1997).
 - [12] M. C. Jullien, P. Castiglione, and P. Tabeling, *Phys. Rev. Lett.* **85**, 3636 (1998).
 - [13] Y. Amarouchene, and H. Kellay, *Phys. Rev. Lett.* **89**, 104502 (2002).
 - [14] H. Kellay and W. I. Goldburg, *Rep. Prog. Phys.* **65**, 845 (2002).
 - [15] O. Greffier, Y. Amarouchene, and H. Kellay, *Phys. Rev. Lett.* **88**, 194101 (2002).
 - [16] R. Bruinsma, *Physica (Amsterdam)* **216A**, 59 (1995).
 - [17] T. Gotoh, J. Nagaki, and Y. Kaneda, *Phys. Fluids* **12**, 155 (2000).
 - [18] G-C. Yuan *et al.*, *Chaos* **10**, 39 (2000); K. Nam *et al.*, *Phys. Rev. Lett.* **83**, 3426 (1999).
 - [19] J. R. Chasnov, *Phys. Fluids* **10**, 1191 (1998).
 - [20] D. Bogucki, J. A. Domaradzki, and P. K. Yeung, *J. Fluid Mech.* **343**, 111 (1997); P. K. Yeung, M. C. Sykes, and P. Vedula, *Phys. Fluids* **12**, 1601 (2000).
 - [21] M. Chertkov *et al.*, *Phys. Rev. E* **51**, 5609 (1995).